Journal of Power Sources 211 (2012) 92–96

Contents lists available at SciVerse ScienceDirect

Journal of Power Sources

journal homepage: www.elsevier.com/locate/jpowsour

Short communication

Hierarchical porous carbon hollow-spheres as a high performance electrical double-layer capacitor material

Yan Han, Xiaoting Dong, Cui Zhang, Shuangxi Liu*

Institute of New Catalytic Materials Science, Key Laboratory of Advanced Energy Materials Chemistry (MOE), College of Chemistry, Nankai University, Tianjin 300071, PR China

ARTICLE INFO

Article history:
Received 9 November 2011
Received in revised form
24 March 2012
Accepted 29 March 2012
Available online 7 April 2012

Keywords:
Carbon hollow-spheres
Hierarchical porous structure
Hydrothermal treatment
Electrochemical performances
Supercapacitor

ABSTRACT

Dispersed carbon hollow-spheres with micropore shells and meso/macropore cores are prepared through a simple and efficient hydrothermal treatment directly using colloidal silica as template. The as-prepared hollow spheres are used as supercapacitor electrode material and exhibit high specific capacitance (about 270 F g^{-1} at 0.5 A g^{-1} in KOH aqueous electrolyte), long cyclic life and excellent rate capability, which is applicable for high performance electrical double-layer capacitors.

1. Introduction

Supercapacitors have received considerable attention because of their high power density, fast recharge capability and long cycle life. Activated carbon is the most widely adopted electrode material. But the slow ion transportation in the small micropores limits their effective utilization [1–3]. Thus, three-dimensionally ordered/aperiodic mesoporous carbons, which facilitate ion transport by providing a smaller resistance and shorter diffusion pathways, could display better performance as supercapacitor electrodes. Recently, many mesoporous carbons with different morphologies and structures have been synthesized and applied as supercapacitor electrode materials, which show high capacitive performance and excellent rate capability [4–8]. However, the typical preparation processes (hard template method) have several limitations such as incomplete infiltration of the carbon precursor and requiring many tedious and time consuming infiltration steps [9–12].

Herein, we report a new route to synthesize dispersed hierarchical porous carbon hollow-spheres directly using colloidal silica as template by hydrothermal treatment. Our strategy offers at least three advantages: (1) the colloidal silica template can be obtained easily by the Stöber method [13,14]; (2) the preparation process directly using colloidal silica as template can be simplified without time consuming infiltration steps; and (3) the deposit thickness of the carbon precursor on the surface of silica spheres is uniform. Furthermore, the electrochemical performances of the carbon hollow-spheres as supercapacitor electrode material are also exploited.

2. Experimental

2.1. Materials synthesis

The synthesis process of carbon hollow-spheres was performed using glucose as carbon source and the amine-modified colloidal silica spheres as hard template that was prepared by Stöber method and surface modified by 3-amino-propyltrimethoxysilane (APMS). More detailed, 0.2 g glucose was dissolved in 20 ml amine-functionalized silica colloid under stirring and hydrothermal treatment at 180 °C for 12 h. The black-brown precipitate was collected and washed with distilled water for several times, and dried at 100 °C for 12 h. Then, the sample was carbonized at 800 °C for 2 h under N_2 flowing. Finally, the silica template was etched using hydrofluoric acid (HF, 40 wt.%).

2.2. Materials characterization

The as-prepared samples were characterized by scanning electron microscopy (SEM, Hitachi TDCLS-4800), transmission

* Corresponding author. Tel./fax: +86 22 23509005.
E-mail address: sxliu@nankai.edu.cn (S. Liu).

0378-7753/$ – see front matter © 2012 Elsevier B.V. All rights reserved.
doi:10.1016/j.jpowsour.2012.03.053

electron microscopy (TEM, Philips Tecnai G^2 F20), Fourier transform infrared spectroscopy (FT-IR, Bruker VECTOR22) and nitrogen adsorption–desorption measurement (Micromeritics ASAP 2020 system at 77 K). The specific surface area (S_{BET}) was calculated from nitrogen adsorption isotherms using the Brunauer–Emmett–Teller (BET) method, whereas the total pore volume was determined by the single point method at $P/P_0 = 0.97$. The pore size distribution (PSD) was analyzed using the density functional theory (DFT) method from the adsorption branch.

2.3. Electrochemical measurement

A conventional three-electrode system was used to evaluate the electrochemical performance. A Ni foil and an Hg/HgO electrode were used as the counter electrode and the reference electrode, respectively. A 6 M KOH aqueous solution was employed as the electrolyte. The working electrode was prepared by pressing the mixture of carbon hollow-spheres, acetylene black and polytetrafluoroethylene (PTFE) with a weight ratio of 90:5:5 onto Ni foam.

The cyclic voltammetry (CV) and electrochemical impedance spectroscopy (EIS) were performed on CHI 660D electrochemical analyzer. The galvanostatic charge/discharge tests were studied using LAND CT2001A instrument.

3. Results and discussion

The overall formation process of the carbon hollow-spheres is illustrated in Fig. 1. First, because there are plenty of cationic ammonium groups ($-\overset{+}{N}H_3$) on the surface of the colloidal silica spheres, the hydroxyl groups (−OH) of the glucose can interact with the positively charged ammonium site electrostatically and be absorbed onto the surface of the silica spheres. Second, the glucose is carbonized preliminarily during hydrothermal treatment and covers such silica sphere surface, which can be confirmed by the FT-IR spectrum of the resulting composite (Fig. 2). As shown in the figure, the absorption bands at about 1620 (together with 1513), 1710 and 3000–2800 cm^{-1} can be assigned to C=C, C=O and C–H stretching vibrations, respectively. The band at about 800 cm^{-1} corresponds to aromatic C–H out-of-plane bending vibration. These indicate dehydration and aromatization processes take place during the hydrothermal carbonization, which are identical to those of the hydrochars [15]. Note that the additional strong bands between 1300 and 1000 cm^{-1} are attributed to skeletal vibrations of the Si–O network derived from the silica sphere. Third, the black-brown carbon/silica composite goes on to be carbonized at 800 °C for 2 h under N_2 to form the porous carbon shell coating on the silica core. Finally, the silica spheres are removed by HF and the carbon hollow-spheres are obtained.

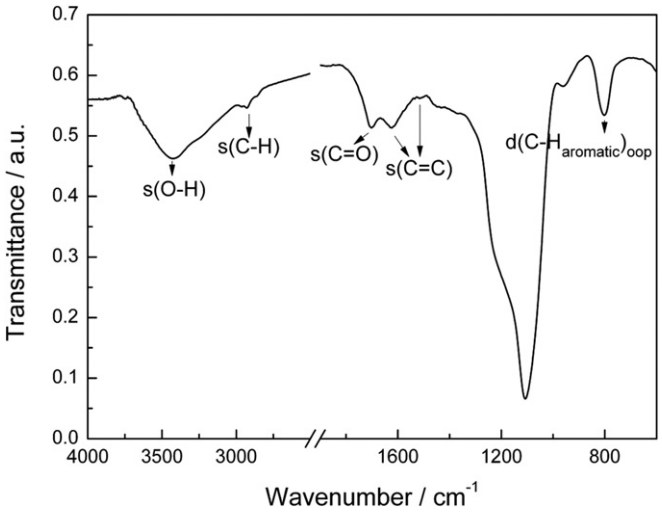

Fig. 2. FT-IR spectrum of the resulting composite after hydrothermal treatment.

The SEM and TEM micrographs of the carbon hollow-spheres are shown in Fig. 3. From the SEM micrograph (Fig. 3a), it can be observed that the sample is composed of dispersed microspheres with a narrow size distribution of around 100 nm. A few cracked spheres with apparent cavities (as pointed out by circles in Fig. 3b) indicate the hollow nature of the as-prepared carbon spheres. Further details of the microstructure of spheres can be seen in the TEM images. As shown in Fig. 3c, the strong contrast between the dark edge and pale center confirms the hollow structure of the carbon spheres. The core size of the carbon spheres is about 40–80 nm, agreed well with the size of colloidal SiO_2 particles (Fig. 1), and the thickness of the shell is about 10 nm. In addition, the high resolution TEM image (Fig. 3d) reveals a disorder microporous texture of the shell, which could result from the emission of small gaseous molecules (H_2O, CO, CO_2) during the carbonization process [16].

The N_2 adsorption–desorption isotherms of the carbon hollow-spheres (shown in Fig. 4a) exhibit combined characteristics of type

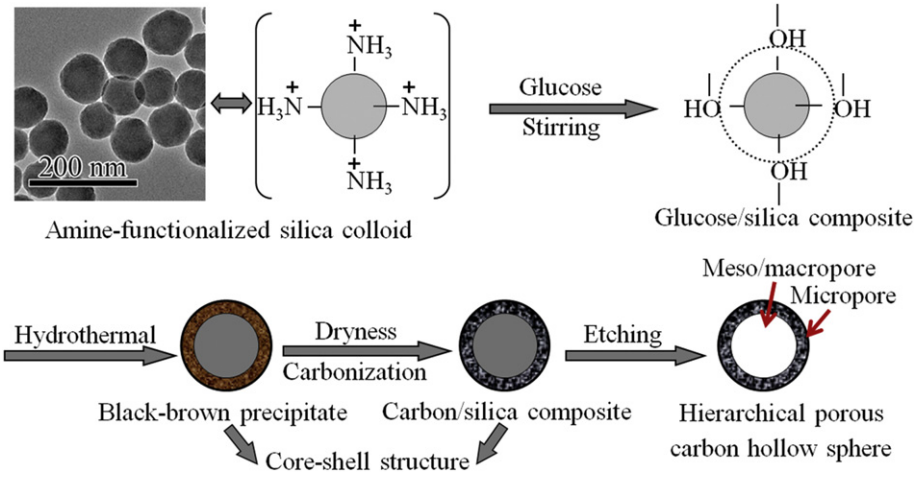

Fig. 1. Schematic illustration of the formation process of the carbon hollow-spheres.

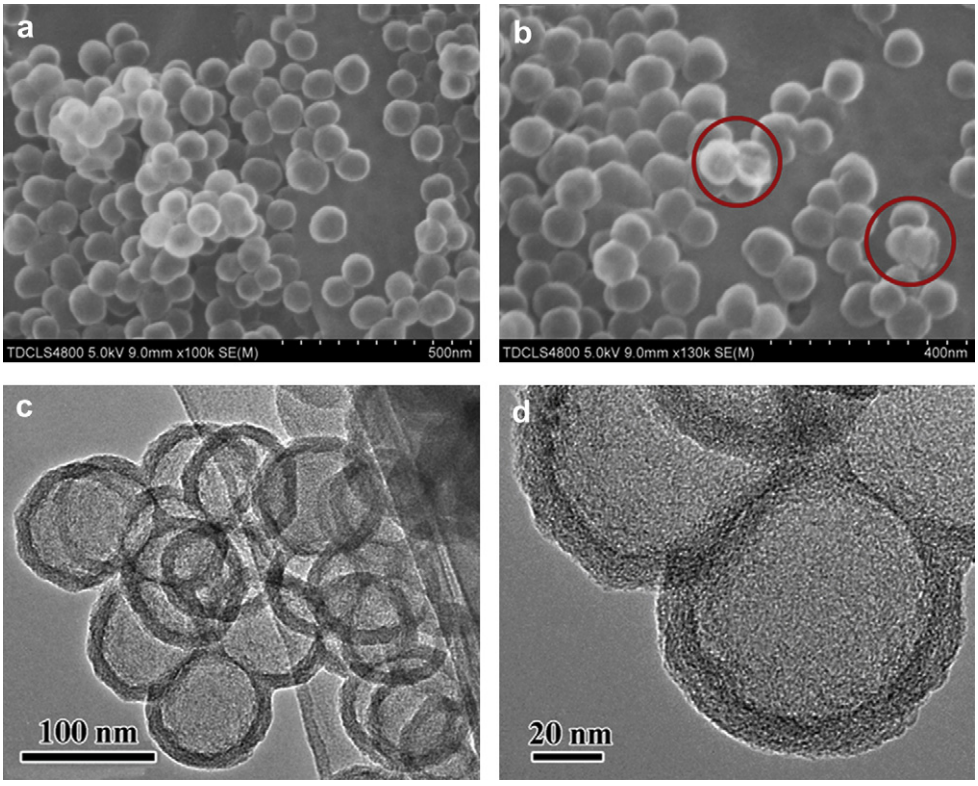

Fig. 3. Representative FESEM (a, b) and TEM (c, d) images of the carbon hollow-spheres.

I/IV, indicating the assembly of micro-, meso- and macropores. The BET specific surface area is 658 $m^2\ g^{-1}$, including a micropore surface area of 318 $m^2\ g^{-1}$ estimated using the t-plot method. And the total pore volume is 1.07 $cm^3\ g^{-1}$. The pore size distribution analyzed using the DFT method is given in Fig. 4b. Three regions can be identified: (1) ultrafine micropores (<1 nm) and micropores (1–2 nm); (2) mesopores (2–50 nm) with a maximum peak at 40 nm; and (3) macropores (>50 nm) with a maximum peak at 68 nm and a minor peak at 150 nm. From the SEM, TEM and N_2 adsorption–desorption results, it can be concluded that the carbon hollow-spheres have a hierarchical porous structure with micropore shell and meso/macropore core, which shows promise as a good electrode material for advanced electrical double-layer capacitors.

The performance of the as-prepared carbon hollow-spheres as supercapacitor electrode material was evaluated by CV, EIS and galvanostatic charge–discharge measurements. The CV curves (Fig. 5a) measured at all voltage scan rates present quasi-rectangular shape, showing a typical characteristic of double-layer capacitance [4,7,16,17]. With the increase of the scan rate, the current gradually increases but the shape of the curves maintains with only slight distortion even at 100 mV s^{-1}. It means that the carbon hollow-spheres exhibit a small equivalent series resistance (ESR) with rapid ion response and the highly capacitive nature [8,17]. The Nyquist plot of the carbon-based electrode (Fig. 5b) shows a straight line in the low frequency region, which is close to those of ideal capacitors. The unconspicuous loop at high frequencies is related to the charge transfer resistance and/or the different contact resistances. The value of ESR obtained from the point intersecting with the real axis is only 0.40 Ω, as shown in the inset of the expanded high frequency region of Fig. 5b. These demonstrate that the carbon hollow-spheres with a hierarchical porous structure can promote the mass transfer/diffusion of ions in to the pores effectively.

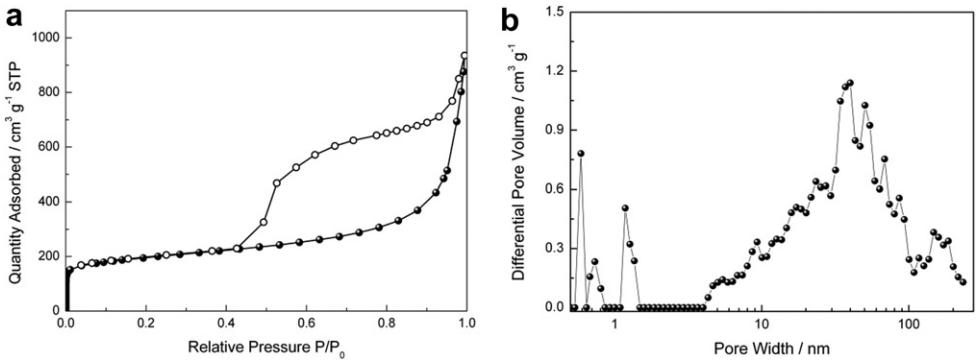

Fig. 4. Nitrogen adsorption–desorption isotherm (a) and pore size distribution (b) of the carbon hollow-spheres.

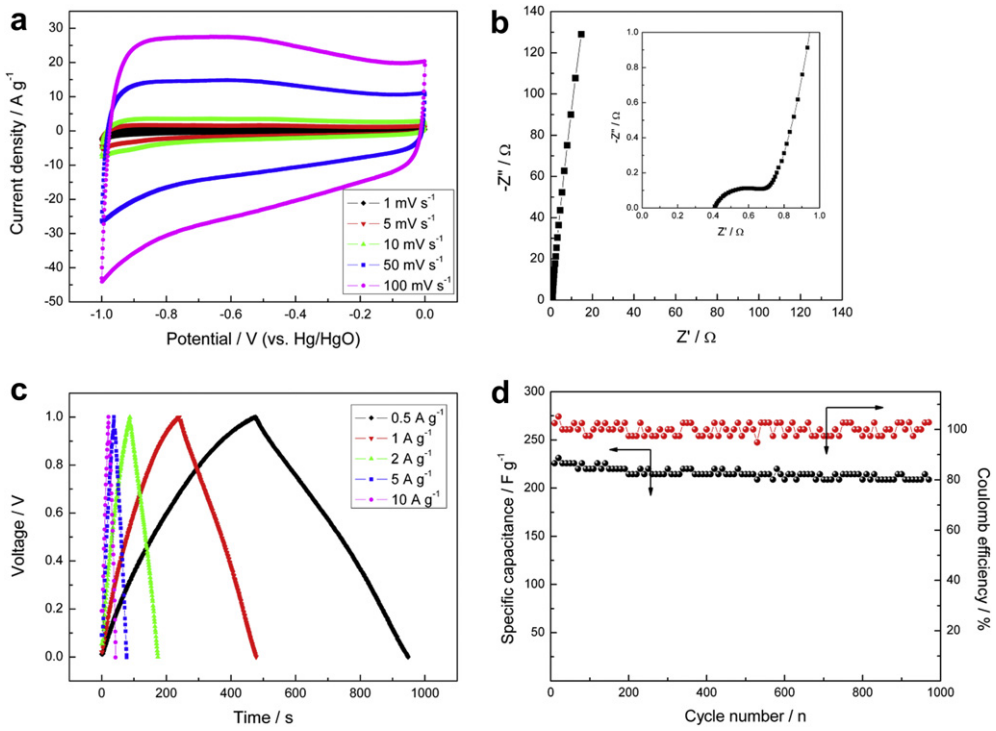

Fig. 5. CV curves at different voltage scan rates (a), Nyquist plot at open circuit potential with amplitude of 5 mV over the frequency range from 100 kHz to 10 mHz (b), plot of potential versus time at different current densities (c) and the variation of specific capacitance with cycle number at 5 A g^{-1} and the corresponding coulomb efficiency (d) for the carbon-base electrodes. The inset in Fig. 4b shows the expanded high frequency region of impedance.

Galvanostatic charge–discharge measurements were conducted to highlight the capacitance characteristic of the carbon hollow-spheres. Fig. 5c shows the plot of voltage versus time at different current densities. As shown in the figure, the charge/discharge curves exhibit almost symmetrical triangle and have not obvious voltage drop (iR) related to the internal resistance during the changing of polarity, showing nearly perfect capacitive behavior. The corresponding specific capacitances of the electrode are calculated on the basis of the equation $C = I\Delta t/(m\Delta V)$, where I is the discharge current (A), Δt is the total discharge time (s), m is the mass of active material on the electrode (g) and ΔV is the potential difference in the discharge process (V). The calculated specific capacitances are 269 F g^{-1} at 0.5 A g^{-1}, 266 F g^{-1} at 1 A g^{-1}, 248 F g^{-1} at 2 A g^{-1}, 220 F g^{-1} at 5 A g^{-1} and 196 F g^{-1} at 10 A g^{-1}, respectively. About 73% of specific capacitance is retained when the charge/discharge rate changes from 0.5 A g^{-1} to 10 A g^{-1}. Obviously, the carbon hollow-spheres exhibit high charge/discharge propagation and excellent rate capability. This is consistent with the CV results and further confirms that the hierarchical porous structure is helpful for ion diffusion with high speed at high current density. The variation of specific capacitance with cycle number at 5 A g^{-1} and the corresponding coulomb efficiency are shown in Fig. 5d. The capacity deterioration is less than 8.0% after 1000 cycles, the coulomb efficiency is almost 100%, which implies the high reversibility and excellent electrochemical stability of the as-prepared porous carbon.

4. Conclusions

In summary, dispersed carbon hollow-spheres were prepared through a simple and efficient hydrothermal treatment using glucose as carbon source and the amine-modified colloidal silica spheres as hard template. SEM, TEM and N_2 adsorption–desorption results confirm that the carbon hollow-spheres have a hierarchical porous structure with micropore shell and meso/macropore core. The electrochemical performances show that the carbon hollow-spheres as supercapacitor electrode material possess superior ion response, high specific capacitance (about 270 F g^{-1} at 0.5 A g^{-1} in KOH aqueous electrolyte), long cyclic life and excellent rate capability, which can be attributed to the unique hierarchical porous structure, not only facilitating fast ion diffusion, offering a good charge accommodation but also reducing the volume change during the charge/discharge cycling.

Acknowledgments

This work was financially supported by National Key Technologies R & D Program of China (2006BAC02A12), National Natural Science Foundation of China (21003077), Natural Science Foundation of Tianjin (08JCZDJC21400) and MOE (IRT-0927).

References

[1] L. Wang, T. Morishita, M. Toyoda, M. Inagaki, Electrochim. Acta 53 (2007) 882–886.
[2] A.G. Pandolfo, A.F. Hollenkamp, J. Power Sources 157 (2006) 11–27.
[3] D. Qu, H. Shi, J. Power Sources 74 (1998) 99–107.
[4] D.W. Wang, F. Li, M. Liu, G.Q. Lu, H.M. Cheng, Angew. Chem. Int. Ed. 47 (2008) 373–376.
[5] F. Li, M. Morris, K.Y. Chan, J. Mater. Chem. 21 (2011) 8880–8886.
[6] B. You, J. Yang, Y.Q. Sun, Q.D. Su, Chem. Commun. 47 (2011) 12364–12366.
[7] F. Xu, R. Cai, Q. Zeng, C. Zou, D. Wu, F. Li, X. Lu, Y. Liang, R. Fu, J. Mater. Chem. 21 (2011) 1970–1976.
[8] Q. Li, R. Jiang, Y. Dou, Z. Wu, T. Huang, D. Feng, J. Yang, A. Yu, D. Zhao, Carbon 49 (2011) 1248–1257.
[9] I. Moriguchi, F. Nakahara, H. Furukawa, H. Yamada, T. Kudo, Electrochem. Solid State Lett. 7 (2004) A221–A223.
[10] H. Yamada, I. Moriguchi, T. Kudo, J. Power Sources 175 (2008) 651–656.
[11] H.N. Hirotoshi Yamada, Fumihiro Nakahara, Isamu Moriguchi, T. Kudo, J. Phys. Chem. C 111 (2007) 227–233.
[12] K. Xia, Q. Gao, J. Jiang, J. Hu, Carbon 46 (2008) 1718–1726.

[13] Y. Han, Y. Wang, Y. Wang, L. Jiao, H. Yuan, Int. J. Hydrogen Energy 35 (2010) 8177–8181.
[14] Y. Chen, H. Kim, Fuel Process. Technol. 89 (2008) 966–972.
[15] M. Sevilla, A.B. Fuertes, Chem. Eur. J. 15 (2009) 4195–4203.
[16] L.L. Zhang, S. Li, J.T. Zhang, P.Z. Guo, J.T. Zheng, X.S. Zhao, Chem. Mater. 22 (2010) 1195–1202.
[17] K. Xie, X.T. Qin, X.Z. Wang, Y.N. Wang, H.S. Tao, Q. Wu, L.J. Yang, Z. Hu, Adv. Mater. 24 (2012) 347–352.